A Simple Method for Detection and Classification of ECG Noises for Wearable ECG Monitoring Devices

Udit Satija, Barathram.Ramkumar and M. Sabarimalai Manikandan
School of Electrical Sciences, Indian Institute of Technology Bhubaneswar
Bhubaneswar, Odisha-751013, India.
Email:{us11,barathram,msm}@iitbbs.ac.in

***Abstract*—An assessment of electrocardiogram (ECG) signal quality has become an unavoidable first step in most holter and ambulatory ECG signal analysis applications. In this paper, we present a simple method for automatically detection and classification of ECG noises. The proposed method consists of four major steps: moving average filter, blocking, feature extraction, and multistage decision-tree algorithm. In the proposed method, the dynamic amplitude range and autocorrelation maximum peak features are extracted for each block. In the first decision stage, a amplitude-dependent decision rule is used for detecting the presence of low-frequency (LF) noise (including, baseline wander (BW) and abrupt change (ABC) artifacts) and the high-frequency (HF) noise (including, power line interference (PLI) and muscle artifacts). In the second decision stage, the proposed method further classifies the LF noise into a BW noise or a ABC noise using the local dynamic amplitude range feature. The HF noise is classified into a PLI noise or a muscle noise using the local autocorrelation maximum peak feature. The proposed detection and classification method is tested and validated using a wide variety of clean and noisy ECG signals. Results show that the method can achieve an average sensitivity (Se) of 97.88%, positive productivity (+P) of 91.18% and accuracy of 89.06%.**

I. Introduction

Recently, wearable cardiac health care monitoring devices enable continuous recording of ECG signals, and early detection and treatment of cardiovascular diseases [1], [2]. Generally, the amplitudes of a normal ECG range from 10 μV to 5 mV and the frequency lies in the range of 0.05-150 Hz [3]. The ECG recordings are generally corrupted by noises, namely, baseline wander (BW), power line interference (PLI), muscle artifact (MA) and instrumentation noise. Furthermore, the motion artifacts is ubiquitous in ECG monitoring using wireless body area networks (WBANs). From the corrupted ECG signals as shown in Fig. 1, it can be noted that the presence of BW, PLI and muscle noises causes inaccurate determination of ECG characteristic points, feature determination, heartbeat segmentation, etc. Thus, assessment of ECG signal quality has become an unavoidable first step in most holter and ambulatory ECG signal analysis applications including cardiac arrhythmias recognition, heart rate variability (HRV) analysis, ECG-based biometric, continuous beat-to-beat blood pressure measurement, sleep apnea detection, and so on. Furthermore, signal quality assessment not only plays an important role in improving diagnostic accuracy of cardiovascular diseases diagnostic systems but also plays in selecting suitable ECG signal enhancement techniques. In addition, wearable ECG monitoring devices hold the promise of continuous recording and early detection of cardiac disease events, but wearable

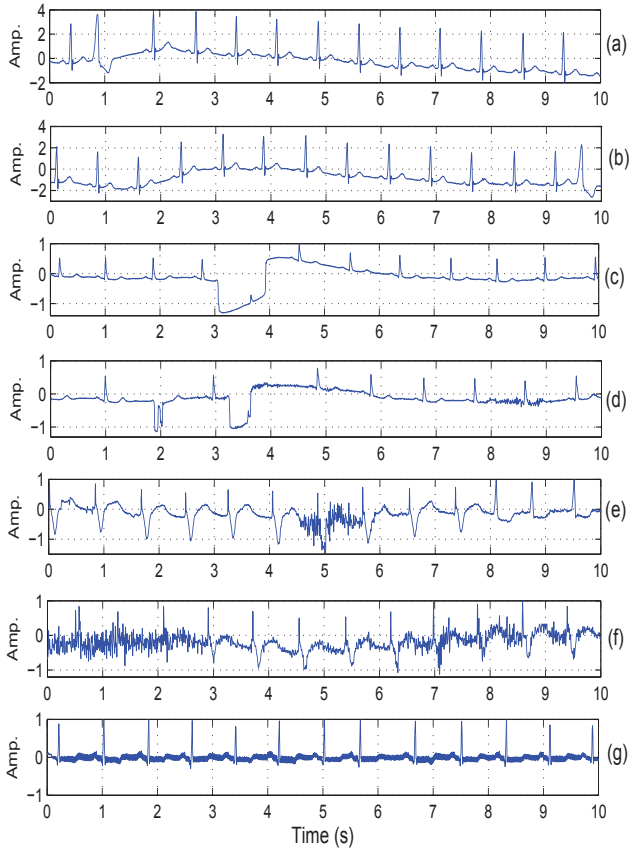

Fig. 1. Illustrates ECG signals corrupted by different types of artifacts and noise: (a) and (b) ECG corrupted with baseline wanders, (c) and (d) ECG corrupted with abrupt changing artifacts, (e) and (f) ECG corrupted with muscle artifacts, and (g) ECG corrupted with PLI noise.

devices have limited power and battery life, limited computational power and main memory. Thus, wearable devices demand energy-efficient reliable ECG noise detection and classification for choosing suitable noise removal technique and guaranteeing clinical acceptability of ECG recordings.

A. Review of ECG Signal Quality Assessment Methods

Many signal quality assessment (SQA) methods have been reported based on statistical features such as mean, standard deviation, kurtosis and heuristic rules. In [4], Orphanidou, et al. presented signal quality indices for ECG and PPG

978-1-4799-5991-4/15/$31.00 ©2015 IEEE

signals using heuristic rules on the extracted features from the QRS or pulse portions and RR intervals, the ratio of maximum to minimum RR interval, and template matching. In [5], SQA method using an artificially reconstructed target lead is presented based on the removal of LF and HF noise, energy-concavity index (ECI) analysis, and a correlation-based examination subroutine calculated between ECG leads estimated by a suitably trained neural network. In [6], L. Johannesen and L. Galeotti presented automatic ECG quality scoring methodology. The method identifies ECG signals with macroscopic errors and subsequently quantifies BW, PLI or muscular noise based on the missing leads, QRS detection, segmentation and erroneous QRS detection. In [7], D. Hayn et al. presented QRS detection based ECG quality assessment based on the empty lead criterion, spike detection criterion, lead crossing point criterion and robustness of QRS detection.

In [8], signal quality indices (SQIs) and data fusion methods were presented for determining clinical acceptability of ECGs. The method consists of spectral energy distribution, higher order moments and inter-channel and inter-algorithm agreement, multi-layer perceptron (MLP) artificial neural network and support vector machine (SVM). In [9], automatic motion and noise artifact detection was presented using empirical mode decomposition (EMD) and statistical approaches. In [10], Hayn et al. presented ECG quality assessment for patient empowerment in m-Health applications. The method is based on basic signal properties (amplitude, spikes, constant signal portions), number of crossing points in between different leads, and QRS amplitude vs. noise-amplitude ratio. In [11], B. E. Moody presented rule-based methods for ECG quality control. In [12], assessment of ECG quality on an android platform was performed based on the lead-fail in all leads, global high frequency noise, leads with noise causing QRS detection problems, global low frequency noise and low and high frequency noise in the beats of sinus origin. Liu et al. presented real-time signal quality assessment for ECGs collected using mobile phones [13]. The method is based on the four flags: misplaced electrode, huge impulse, strong Gaussian noise, error of R-wave peaks by the template matching. Based on the values of four flags, single signal quality index (SSQI) and integrative signal quality index (ISQI) were computed for single lead ECG and twelve-lead ECGs, respectively. In [14], simple scoring system for ECG quality assessment on android platform. In [15], a new ABP signal quality index (SQI) was presented for measuring morphological normality and degradation due to noise. Most existing SQA methods were validated using datasets available in Physionet/Computing in Cardiology Challenge 2011 (PICC2011) [18].

B. Limitations of Existing SQA Methods

Many QRS detection based SQA methods were proposed by analyzing the detected R-R intervals from the input ECG signal. The detection of exact R-R interval (or heart rate) is severely affected in the cases of clean ECG signal with (i) wide QRS complexes, (ii) low-amplitude QRS complexes, (iii) negative QRS polarities, (iv) sudden changes in RR intervals, (v) sudden changes in QRS amplitudes, (vi) sudden changes in QRS morphologies, and (vii) sharp P- and T-waves [22],[23]. Under this scenarios, the existing heart rate ECG signal quality assessment methods demand accurate detection of time-instants of R-peaks present in the ECG signal. Most methods use traditional R-peak detection (or waveform delineation) algorithm, which had poor detection rates in case of ECG signals. Furthermore, most detection methods include sets of amplitude-dependent, duration-dependent and interval-dependent thresholds for to detect R-peaks, and to reject or include noise and missed R-peaks. The searchback algorithm with two rules with adaptive amplitude-dependent and time-dependent thresholds were widely adopted to reject or include identified R-peaks located at t_m and t_n: $i)$ if $t_n - t_m < 0.2\ s$ (refractory period) and $ii)$ search back if $t_n - t_m > 1.5\mathrm{RR}_{\mathrm{avg}}$. These rules may improve detections for regular rhythms but some rules may be in conflict with others. Furthermore, searchback mechanism cannot be halted in case of irregular rhythms with varying QRS complexes. Moreover, there are often lots of thresholds defined in heuristic rules [22]. In most approaches, the detection thresholds were adapted based on past detected R-peaks. In such a case, detection performance highly depends on the accurate estimation of initial thresholds at the learning phase.

In EMD based methods, local waves of ECG signal and noises are distributed over a number of intrinsic mode functions (IMFs). Under this scenario, it is difficult to determine the noisy IMFs from the signal IMFs. Although the frequency range of each wavelet subband is known, the wavelet coefficients of BW, PLI, and MA noises and ECG signal are spread over detail and approximation subbands. Thus, noise subband characterization can be difficult under time-varying PQRST morphologies and noise characteristics. However, we cannot fix the wavelet filter, number of decomposition level and characteristic subbands. Thus, developing low-complexity automated ECG signal quality assessment method is still a challenging research problem.

C. Contribution of this Paper

In this paper, we present a simple straightforward ECG noise detection and classification method. The proposed method consists of four major stages: moving average filtering, blocking, feature extraction, and multi-stage decision classification. In the proposed method, the features such as global and local dynamic amplitudes and autocorrelation maximum peak are extracted in this work. Based on these features, the multi-stage decision stage is constructed automatic detection and classification of ECG noises. Experimental results show that the method achieves an acceptable classification accuracy on different types of clean and noisy ECG signals.

The rest of this paper is organized as follows. The proposed ECG noise detection and classification method is described in Section II. In Section III, the performance of the proposed method is tested and validated using a wide variety of clean and noisy ECG signals. Finally, conclusions are drawn in Section IV.

II. Proposed ECG Noise Detection and Classification Method

In this Section, we present a simple straightforward method for automatically detection and classification of ECG noises. The proposed method consists of four major stages: signal suppression and noise enhancement, feature extraction, amplitude-dependent detection and decision-tree based noise classification.

A. ECG Signal Suppression and Noise Enhancement

In this work, the proposed method implements a moving average filter for obtaining the low-frequency (LF) component part including the BW noises and the high-frequency (HF) component part including the PLI, muscle artifacts and recording instrument noise. In this work, the filtering step process the 10 s ECG signal $x[n]$. For extracting the baseline wander noise (or low-frequency (LF) artifacts) from the input ECG signal, the moving average filter is implemented as

$$\mathbf{u}[n] = \frac{1}{L+1}\sum_{k=0}^{L}\mathbf{x}[n-k] \tag{1}$$

where L denotes the moving average filter length. In this work, the filter length is chosen such that it can adequately capture the BW noise below 0.5 Hz. The high-frequency (HF) noise including the PLI, muscle artifacts and recording instrument noise from the input ECG signal is extracted using the difference equation as

$$\mathrm{v}_1[n] = \frac{1}{L+1}\sum_{k=0}^{L}\mathbf{x}[n-k] \tag{2}$$

$$\mathrm{v}[n] = \mathrm{x}[n] - \mathrm{v}_1[n], \qquad n = 0, 1, 2....., N-1. \tag{3}$$

The filter length for the moving average filter II is chosen such that it can adequately capture the ECG signal below 40 Hz. In order to avoid phase lags, the filtering operation is implemented using zero-phase filtering process with filter coefficients $b_k = 1, \quad k = 0, 1, 2, 3, ...L-1$. Then, the noise signal features are extracted from both LF component and HF component parts for detecting the presence of BW, PLI, muscle artifacts and recording instrument noises. The output waveforms as shown in Fig. 2 (b) and (d) show the LF component and HF component parts obtained for the ECG signal corrupted with BW noise.

B. Feature Extraction Stage

The feature extraction stage is implemented based on the following steps: non-overlapping blocking and feature computation. In the blocking process, the filtered signal is divided into non-overlapping blocks with block duration of 200 ms. In this work, the kth block $\mathbf{u}_k(n)$ of $\mathbf{u}(n)$ is obtained as

$$\mathbf{u}_k[n] = \mathbf{u}[\mathrm{P}k+n] \quad n = 1, 2, \cdots \mathrm{P} \tag{4}$$

where $k = 0, 1 \cdots \mathrm{M}-1$, $\mathrm{M} = \lfloor \frac{\mathrm{N}}{\mathrm{P}} \rfloor$ and P denotes the size of the window. For each processing window, the maximum and minimum values are computed for discriminating the background noise level which can mask the low-amplitude local waves of the PQRST morphologies. In this work, the maximum and minimum amplitude values of each window are computed as

$$\begin{aligned} a_{\max}[k] &= \max\{u_k[n]\} \quad k = 0, 1 \cdots \mathrm{M}-1 \\ a_{\min}[k] &= \min\{u_k[n]\} \quad k = 0, 1 \cdots \mathrm{M}-1 \end{aligned} \tag{5}$$

For detecting the presence of BW noises, the dynamic amplitude range of each window is compared with the predefined amplitude threshold. The dynamic amplitude range is computed as

$$a_{\mathrm{dr}}[k] = a_{\max}[k] - a_{\min}[k] \quad k = 0, 1, 2 \cdots \mathrm{M}-1 \tag{6}$$

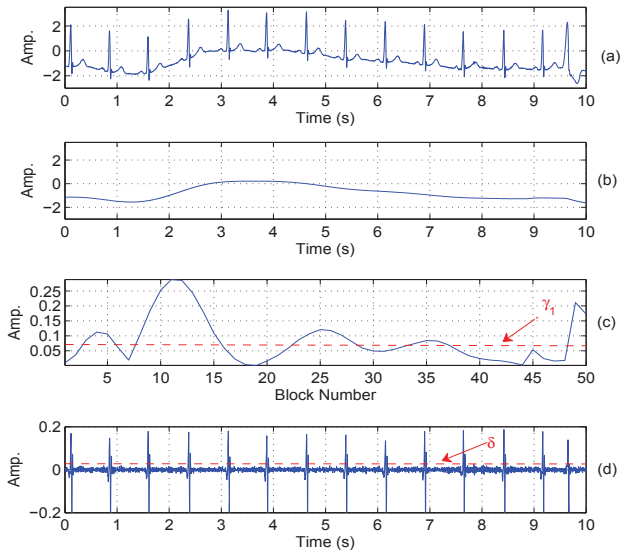

Fig. 2. Illustrates the feature signals obtained for the ECG signal with BW noise. (a) Corrupted ECG signal, (b) Extracted LF component part including BW noise, (c) dynamic amplitude range estimates, and (d) high-frequency (HF) component part.

The output waveforms of each step of the feature extraction stage are shown in Fig. 2. The LF component part in Fig. 2(b) contains the BW noise with larger amplitude variation. In order to discriminate the BW noise from the abrupt change artifacts, the local dynamic amplitude range is estimated for each window. The output of the dynamic amplitude range estimator for the LF component part is shown in Fig. 2 (c). By implementing the amplitude thresholding rule with a predefined threshold γ_1, $a_{dr}[k] > \gamma_1$, the BW noise event is distinguished from the abrupt change artifacts by determining low-magnitude frame ratio.

TABLE I. ECG LOCAL WAVES AND THEIR CHARACTERISTIC PARAMETERS [19], [20]

ECG Waves	Amplitude Range	Duration
P wave	0.1-0.2 mV	100 ms
QRS complex	$0.5 - 1.0$ mV	$80 - 100$ ms
T wave	≈ 0.5 mV	$150 - 200$ ms
U wave	$1 - 2$ mm or 25 % of T wave height	-

For detecting the presence of HF noise components such as PLI and muscle noises, the HF component part $\mathbf{v}(n)$ is obtained using equation (3). The order of the filter is chosen such that the 50/60 Hz PLI and muscle noises are captured in the HF component part. For a test ECG signal corrupted with BW noise, the extracted HF component part is shown in Fig. 2(d). It is observed that the HF component not only contains low-amplitude high-frequency background noise but also includes components of QRS complexes. In this work, the influence of the high-frequency noises is first detected by comparing the estimated maximum value of the absolute of HF component with a predefined amplitude threshold δ, which is found based on the amplitudes of local waves of the ECG signal as shown in Table I. Based upon the amplitudes of local waves, the amplitude threshold δ is chosen. The low-amplitude PLI and muscle noises may be removed by

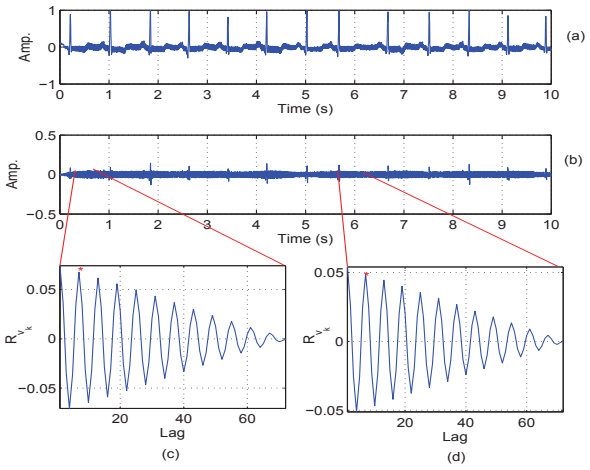

Fig. 3. Illustrates the existence of periodicity of the signal block obtained from the HF component part including the PLI noise. (a) ECG signal corrupted with PLI noise, (b) Extracted HF component including the PLI noise and high-frequency component of the QRS complexes in the ECG signal, (c) AC sequence obtained for block of samples taken from between first R-peak and second R-peak, and (d) AC sequence obtained for the eighth and ninth R-peaks.

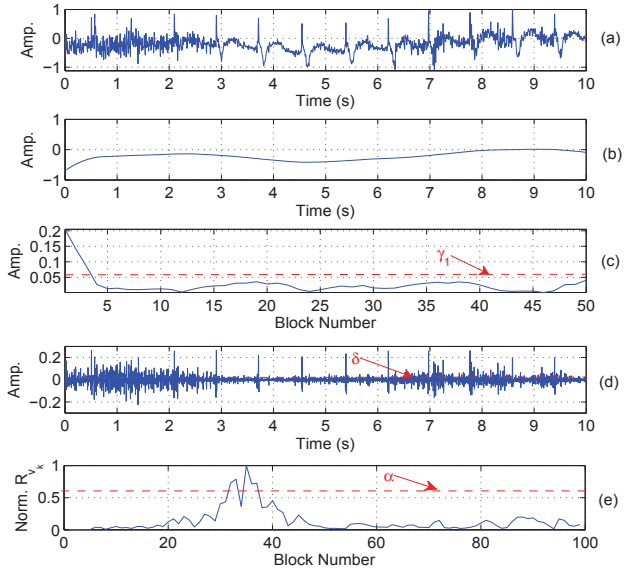

Fig. 4. Illustrates the feature signals obtained for the ECG signal with muscle artifacts. (a) Corrupted ECG signal, (b) Extracted LF component part including BW noise, (c) dynamic amplitude range estimates, (d) high-frequency (HF) component part and (e) ACF feature signal obtained using maximum peak value of the ACF function.

using a simple smoothing filter. The method assumes that the high-amplitude PLI and muscle noises can mask the fiducial points (onsets, offsets, peaks) of the medium amplitude local waves (including, P, q, T, and U). In this work, the acceptable background noise level is chosen such that the fiducial points can be preserved after applying noise removal techniques. The amplitude threshold δ of 0.02 mV is chosen. For detecting the presence of HF noise part, we estimate the total number of samples ($\mathrm{N_{HF}}$) that are above the δ=0.02 mV. If the estimated $\mathrm{N_{HF}} > 2 \times \mathrm{F}_s$ then the method labels the presence of HF noise part.

Once the presence of the HF noise part is identified then the HF noise is further processed to classify the HF noise part into a PLI noise or a muscle noise. In the HF noise classification process, the HF component part is segmented into overlapping blocks with duration of 200 ms with block shift (Q) of 100 ms. The overlapping blocking process is implemented as

$$\mathbf{v}_k[n] = \mathbf{v}[\frac{\mathrm{P}k}{2} + n] \quad n = 1, 2, \cdots \mathrm{P} \tag{7}$$

where $k = 0, 1 \cdots \mathrm{M}_1 - 1$ and $\mathrm{M}_1 = \lfloor \frac{\mathrm{N}}{\mathrm{Q}} \rfloor$. In this work, the autocorrelation features are used for discriminating the structured PLI noise from the muscle noise. In our previous work, the effectiveness of the autocorrelation function in determining the periodicity of the signal [24]. For each block $\mathbf{v}_k[n]$, the autocorrelation sequence is computed as

$$\mathbf{R_k}(\tau) = \frac{1}{\mathrm{P}} \sum_{n=0}^{\mathrm{P}} \mathbf{v}_k[n]\mathbf{v}_k[n+\tau] \tag{8}$$

where $\mathbf{R_k}(\tau)$ denotes the autocorrelation function (ACF) for $\mathbf{v}_k[n]$ and τ denotes the autocorrelation lag. With reference to the first negative zerocrossing point, the global maximum of the autocorrelation function is estimated for each block. The results of the autocorrelation function are shown in Fig. 3 for visual inspection. The autocorrelation plots show that the existence of the structured PLI noise. The effectiveness of the ACF function is further evaluated using the ECG signals corrupted with muscle artifacts and PLI noise. The output waveforms of the autocorrelation feature extraction stage are shown in Figs. 4 and 5. For these two noisy ECG signals, the LF component parts show low-amplitude BW noise component which is less than the BW noise amplitude threshold γ_1. The HF component parts for the ECG signals corrupted with muscle artifacts and PLI noise are shown in Figs. 4(d) and 5(d), respectively. The ACF feature signals are shown in Figs. 4(e) and 5(e). From the ACF signal as shown in Fig. 4(e), it is noted that the most signal blocks have maximum peak value below 0.2. From this experiment, we notice that most blocks from the muscle artifact part have poor intra-block correlation. Meanwhile, the ACF result in Fig. 5(e) shows that most blocks have maximum peak value above 0.4. By selecting the suitable autocorrelation peak threshold, the HF component part is classified into a PLI noise and a muscle noise. A simplified multi-stage decision based noise detection and classification method is shown in Fig. 6.

III. Results and Discussion

In this Section, we evaluate the performance of the proposed detection and classification method using a wide variety of ECG signals including different kinds of PQRST morphologies and various kinds of artifacts and noise including baseline wander (BW), abrupt change (ABC) artifacts, power line interference (PLI) and muscle artifacts. In this work, the first decision stage first detects the presence of the low-frequency (LF) noise (including, baseline wander (BW) and abrupt change (ABC) artifacts) and the high-frequency (HF) noise (including, power line interference (PLI) and muscle artifacts). In the second decision stage, the LF component and HF component parts are further classified into any of the BW,

TABLE II. COMPARISON BETWEEN GROUND TRUTH AND THE PROPOSED CLASSIFICATION METHOD FOR DIFFERENT ECG NOISE CASES.

Record	Ground Truth Annotation									Classification Results								
	Clean	BW	ABC	MN	PL	BW+PL	BW+MN	ABC+PL	ABC+MN	Clean	BW	ABC	MN	PL	BW+PL	BW+MN	ABC+PL	ABC+MN
100	9	66	21	5	23	1	25	0	0	8	62	25	6	20	4	24	1	0
101	2	74	9	0	4	14	43	2	2	3	85	15	0	2	10	34	0	1
102	4	68	23	0	26	0	29	0	0	8	70	25	3	20	5	15	1	3
103	6	74	16	15	23	1	15	0	0	4	71	20	21	21	5	8	0	0
104	3	41	7	5	5	10	73	0	6	2	34	5	8	3	8	81	0	9
105	6	66	18	0	24	2	34	0	0	9	61	15	1	28	3	32	0	1
106	19	55	13	15	18	6	21	0	3	17	51	15	15	20	8	23	0	1
107	18	111	8	0	5	8	0	0	0	20	108	11	4	4	3	0	0	0
108	4	23	18	1	4	11	86	0	3	1	15	14	9	3	10	91	1	6
109	11	72	19	16	17	1	14	0	0	14	75	17	14	14	1	15	0	0
111	4	77	7	6	7	15	33	0	1	2	82	10	8	3	11	34	0	0
Total	**86**	**727**	**159**	**63**	**156**	**69**	**373**	**2**	**15**	**88**	**714**	**172**	**89**	**138**	**68**	**357**	**3**	**21**

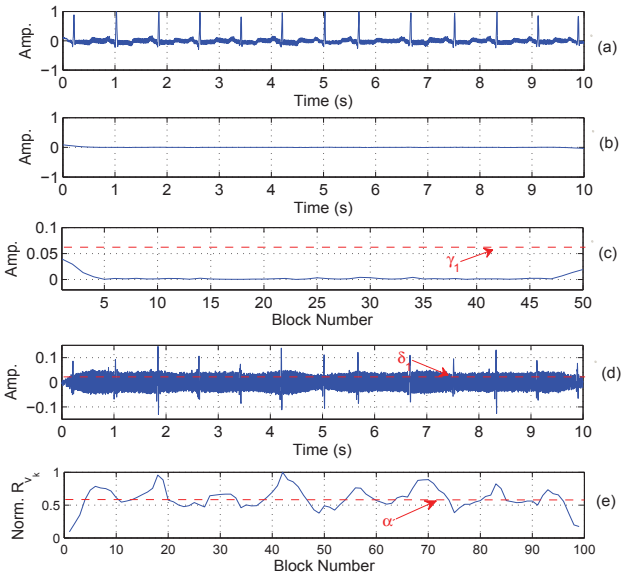

Fig. 5. Illustrates the feature signals obtained for the ECG signal with PLI noise. (a) Corrupted ECG signal, (b) Extracted LF component part including BW noise, (c) dynamic amplitude range estimates, (d) high-frequency (HF) component part and (e) ACF feature signal obtained using maximum peak value of the ACF function.

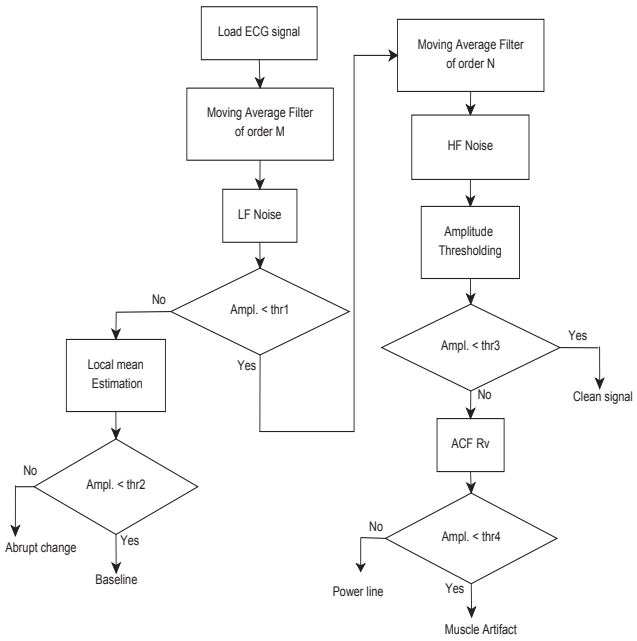

Fig. 6. A simplified flowchart of the proposed ECG noise detection and classification method.

ABC, PLI, and muscle noise classes. A simplified flowchart of the proposed ECG noise detection and classification method is shown in Fig. 6.

For performance evaluation purposes, a large scale of test ECG signal database is created using ECG signals taken from records of the MIT-BIH Arrhythmia Database (mitadb) [17]. The ECG signals were sampled at rate of 360 Hz and quantized with resolution of 11-bit. The test ECG database has 150 ECG signals. The duration of each test ECG signal is 10 s. A large scale of test ECG database is created by adding various kinds of noises with different noise levels. The synthetic noises are generated using the software package available in [21]. The ground-truth annotation results are summarized in Table II for all classes of noise.

For performance validation, the three benchmark parameters such as sensitivity (Se), positive predicitivity (+P) and accuracy are computed as

$$Se = \frac{\mathrm{TP}}{\mathrm{TP} + \mathrm{FN}} \times 100 \tag{9}$$

$$+P = \frac{\mathrm{TP}}{\mathrm{TP} + \mathrm{FP}} \times 100 \tag{10}$$

$$Accuracy = \frac{\mathrm{TP}}{\mathrm{TP} + \mathrm{FN} + \mathrm{FP}} \times 100 \tag{11}$$

where TP denotes the true positive (TP) which is defined the test segment is correctly classified by the algorithm, FP denotes the false positive defined as the the test segment is falsely classified as a particular noise type, and FN denotes the false negative defined as the test segment is misclassified as other noise type. Table III summarizes the performance of the proposed method in terms of benchmark parameters such as sensitivity (Se), positive predicitivity (+P) and accuracy. The method achieves a classification accuracy above 85% for most noise types, except for the mixture noise classes: ABC plus PLI and ABC plus muscle artifacts. The confusion matrix for the classification method is shown in Table IV. Based upon the results shown in Table III and Table IV, it is noted that the proposed method can suitable for detecting most commonly encountered noise types including BW, PLI, ABC and muscle

TABLE III. CLASSIFICATION RESULTS OF THE PROPOSED METHOD

Signal Type	Total No. of Segments	TP	FP	FN	Se (%)	+P (%)	Accuracy (%)
Clean	86	86	2	-	100	97.72	97.72
BW	727	714	-	13	98.21	100	98.21
ABC	159	159	13	-	100	92.44	92.44
MN	63	63	26	-	100	92.44	92.44
PL	156	138	-	18	88.46	100	88.46
BW+PL	69	68	-	1	98.55	100	98.55
BW+MN	373	357	-	16	95.71	100	95.71
ABC+PL	2	2	1	-	100	66.66	66.66
ABC+MN	15	15	6	-	100	71.42	71.42
Total	**1650**	**1602**	**48**	**48**	**97.88**	**91.18**	**89.06**

TABLE IV. CONFUSION MATRIX RESULT FOR THE PROPOSED CLASSIFICATION METHOD

	Clean	BW	ABC	MN	PL	BW+PL	BW+MN	ABC+PL	ABC+MN
Clean	86	2	-	-	-	-	-	-	-
BW	3	714	-	2	-	-	8	-	-
ABC	-	3	159	-	-	-	6	-	4
MN	-	-	4	63	2	-	14	-	6
PL	-	-	-	7	138	9	-	2	-
BW+PL	-	-	-	-	-	68	1	-	-
BW+MN	-	-	-	8	-	-	357	-	8
ABC+PL	-	-	-	1	-	-	-	2	-
ABC+MN	-	-	-	-	-	-	5	1	15

artifacts and mixture noise types including BW plus PLI, and BW plus muscle artifacts.

In the future directions, we further study the performance of the proposed detection and classification method using the other mixture of noise types. The proposed method uses simple filtering, feature extraction and classification techniques as compared with signal decomposition and feature extraction techniques and supervised classifiers of the existing noise detection and classification methods. The wearable cardiac monitoring devices highly demand a low-complexity signal quality assessment method since these wearable medical devices have limited battery power, memory space and computational speed. Based on the classification results, we believe that the proposed method is suitable for assessing the quality of ECG recordings in holter and ambulatory monitoring applications.

IV. CONCLUSION

In this paper, we present a simple method for automatically detection and classification of ECG noises. The proposed method consists of four major steps: moving average filter, blocking, feature extraction, and multistage decision-tree algorithm. In the proposed method, the features including the global and local dynamic amplitude ranges and autocorrelation maximum peak extracted for detection and classification of ECG noises. The proposed detection and classification method is tested and validated using a wide variety of clean and noisy ECG signals. Results show that the method can achieve an average sensitivity (Se) of 97.88%, positive productivity (+P) of 91.18% and accuracy of 89.06%. Unlike other existing methods, the proposed method uses simple filtering, feature extraction and classification techniques.

REFERENCES

[1] A. Pantelopoulos, N. G. Bourbakis, "A survey on wearable sensor-based systems for health monitoring and prognosis," *IEEE Trans. Syst. Man Cybern. C, Appl. Rev.*, vol. 40, no. 1, pp. 1-12, 2010.

[2] S. Movassaghi, M. Abolhasan, J. Lipman, D. Smith, and A. Jamalipour, "Wireless body area networks: A survey," *IEEE Commun. Surveys Tutorials*, Accepted, 2014.

[3] P. Kligfield *et al.*, "Recommendations for the standardization and interpretation of the electrocardiogram: part I: the electrocardiogram and its technology," *J. of the American College of Cardiol.*, vol. 49, no. 10, pp. 1109-1127, 2007.

[4] C. Orphanidou, et al., "Signal quality indices for the electrocardiogram and photoplethysmogram: derivation and applications to wireless monitoring," *IEEE J. of Biomed. and Health Informatics*, 2014.

[5] H. Naseri, M. R. Homaeinezhad, "Electrocardiogram signal quality assessment using an artificially reconstructed target lead," *Computer methods in Biomechanics and Biomed. Eng.*, In press, pp. 1-16, 2014.

[6] L. Johannesen, L. Galeotti, "Automatic ECG quality scoring methodology: mimicking human annotators," *Physiological Meas.*, vol. 33, no. 9, pp. 1479-1490, 2012.

[7] D. Hayn, B. Jammerbund, and G. Schreier, "QRS detection based ECG quality assessment," *Physiological Meas.*, vol. 33, no. 9, pp. 1449-1462, 2012.

[8] G. D. Clifford, J. Behar, Q. Li, and I. Rezek, "Signal quality indices and data fusion for determining clinical acceptability of electrocardiograms," *Physiological Meas.*, vol. 33, no. 9, pp. 1419-1437, 2012.

[9] J. Lee, D. D. McManus, S. Merchant, K. H. Chon, "Automatic motion and noise artifact detection in Holter ECG data using empirical mode decomposition and statistical approaches," *IEEE Trans. on Biomed. Eng.*, vol. 59, no. 6, pp. 1499-1506, 2012.

[10] D. Hayn, B. Jammerbund, G. Schreier, "ECG quality assessment for patient empowerment in mHealth applications." *Comput. Cardiol.*, pp. 353-356, Sept. 2011.

[11] B. E. Moody, "Rule-based methods for ECG quality control," *Comput. Cardiol.*, vol. 38, pp. 361-3, 2011.

[12] L. Johannesen, "Assessment of ECG quality on an android platform," *38th Physionet Cardiol. Challenge*, 2011.

[13] C. Liu, P. Li, L. Zhao, F. Liu, and R. Wang, "Real-time signal quality assessment for ECGs collected using mobile phones," *IEEE Comput. Cardiol.*, pp. 357-360, Sep. 2011.

[14] V. Chudacek, L. Zach, J. Kuzilek, J. Spilka, and L. LhotskA, "Simple scoring system for ECG quality assessment on android platform," *Comput. Cardiol*, pp. 449-451, Sep. 2011.

[15] Q. Li, R. G. Mark, and G. D. Clifford, "Artificial arterial blood pressure artifact models and an evaluation of a robust blood pressure and heart rate estimator," *Biomed. Eng. online*, vol. 8, no. 1, 2009.

[16] S. J. Redmond, N. H. Lovell, J. Basilakis, and B. G. Celler, "ECG quality measures in telecare monitoring," *Eng. Medicine and Biology Soc., 2008. EMBS 2008. 30th Annual Int. Conf. IEEE*, pp. 2869-2872, Aug. 2008.

[17] http://physionet.org/physiobank/database/mitdb/

[18] http://physionet.org/challenge/2011/

[19] J. R. Hampton, "The ECG Made Easy," *Elsevier Health Sciences*, 2013.

[20] R. M. Rangayyan, "Biomedical signal analysis," *IEEE Standards Office*, 2001.

[21] P.E. McSharry, G.D. Clifford, ECGSYN-a realistic ECG waveform generator (http://www.physionet.org/physiotools/ecgsyn/

[22] P. Kathirvel, M. Sabarimalai Manikandan, S. R. M. Prasanna, and K. P. Soman, "An efficient R-peak detection based on new nonlinear transformation and first-order Gaussian differentiator," *Cardiovascular Eng. and Technology*, vol. 2, no. 4, pp. 408-425, 2011.

[23] M. Sabarimalai Manikandan and B. Ramkumar, "Straightforward and robust QRS detection algorithm for wearable cardiac monitor," *Healthcare Technology Lett.*, vol. 1, no. 1, pp. 40-44, 2014.

[24] M. S. Manikandan, and K. P. Soman, "Robust heart sound activity detection in noisy environments," *Elect. Lett.*, vol. 46, no. 16, pp. 1100-1102, 2010.